Published in final edited form as:
J Cell Biochem. 2012 June ; 113(6): 1955–1965. doi:10.1002/jcb.24064.

Pro-apoptotic gene knockdown mediated by nanocomplexed siRNA reduces radiation damage in primary salivary gland cultures

Szilvia Arany[1], **Qingfu Xu**[2], **Eric Hernady**[3], **Danielle S.W. Benoit**[4], **Steve Dewhurst**[2], and **Catherine E. Ovitt**[1]

[1]Center for Oral Biology, University of Rochester School of Medicine and Dentistry, Rochester, NY, USA

[2]Department of Microbiology and Immunology, University of Rochester School of Medicine and Dentistry, Rochester, NY, USA

[3]Department of Radiation Oncology, James P. Wilmot Cancer Center, University of Rochester, NY, USA

[4]University of Rochester, Department of Biomedical Engineering and Chemical Engineering, Rochester, NY, USA

Abstract

A critical issue in the management of head and neck tumors is radioprotection of the salivary glands. We have investigated whether siRNA-mediated gene knock down of pro-apoptotic mediators can reduce radiation-induced cellular apoptosis in salivary gland cells in vitro. We used novel, pH-responsive nanoparticles to deliver functionally active siRNAs into cultures of salivary gland cells. The nanoparticle molecules are comprised of cationic micelles that electrostatically interact with the siRNA, protecting it from nuclease attack, and also include pH-responsive endosomolytic constituents that promote release of the siRNA into the target cell cytoplasm. Transfection controls with Cy3-tagged siRNA/nanoparticle complexes showed efficiently internalized siRNAs in more than 70% of the submandibular gland cells. We found that introduction of siRNAs specifically targeting the Pkcδ or Bax genes significantly blocked the induction of these pro-apoptotic proteins that normally occurs after radiation in cultured salivary gland cells. Furthermore, the level of cell death from subsequent radiation, as measured by caspase-3, TUNEL, and mitochondrial disruption assays, was significantly decreased. Thus, we have successfully demonstrated that the siRNA/ nanoparticle-mediated knock down of pro-apoptotic genes can prevent radiation-induced damage in submandibular gland primary cell cultures.

Keywords

irradiation; salivary gland; apoptosis; Pkcδ; Bax; in vitro

Head and neck cancers account for 3–5% of all cancers worldwide and their treatment generally involves the use of ionizing radiation, which results in subsidiary, permanent damage to the salivary glands [O'Connell et al., 1999; Vissink et al., 2003]. The mechanism

Corresponding author: Szilvia Arany and Catherine E. Ovitt, Center for Oral Biology, University of Rochester Medical Center, 601 Elmwood Avenue, Box 611, Rochester, NY 14642, USA, Tel: (585) 275-2920, Fax: (585) 276-0190, szilvia_arany@urmc.rochester.edu, catherine_ovitt@urmc.rochester.edu.

behind apoptosis of the salivary gland cells following irradiation has been intensively reviewed [Grundmann et al., 2009; Stephens et al., 1991b] and is a complex, "enigmatic" process [Nagler, 2002]. Although the serous components of the acini (functional units of the salivary glands) are postmitotic, highly-differentiated cells, they exhibit prominent radiosensitivity [Stephens et al., 1991a]. Irradiation-induced cell death and subsequent tissue destruction has been explained by the "granulation hypothesis" [Nagler et al., 1997], plasma membrane damage [Takagi et al., 2003], disruptions in signal-transduction [Vissink et al., 1992], and DNA damage in the progenitor cells [Konings et al., 2005]. Overall, radiation damage results in a complex manifestation of apoptosis, necrosis, mitotic catastrophe, and autophagy [Eriksson and Stigbrand, 2010], and major cellular loss is attributed principally to apoptosis [Redman, 2008]. Taken together, the final outcome is severe functional impairment of the salivary glands, and management of the resulting hyposalivation represents a demanding and unresolved clinical challenge.

Radioprotection and therapeutic treatments have addressed various aspects of this problem. Symptomatic treatments with sialogogues offer only palliative, temporary relief. The use of chemo- or radio-protective agents (e.g. amifostine) prior to radiation leads to severe side effects [Jensen et al., 2010]. Sparing the salivary glands from radiation effects by using novel, intensity modulated [Braam et al., 2006] or fractionated radiotherapy, as well as chemo-radiotherapy represents a preventive approach. Unfortunately, this protection method is case sensitive and technology dependent [Seiwert et al., 2007]. Numerous investigations, *in vitro* and *in vivo* have evaluated the possible efficacy of anti-apoptotic agents. Reduction of cellular apoptosis through extrinsic growth factors (IGF-1 [Limesand et al., 2009], or bFGF [Thula et al., 2005]) has shown promising results, but their wide-ranging systemic effects may also pose problems. Heat shock protein 25 has been suggested to protect acinar cells from radiation stress *in vivo* [Lee et al., 2006], but it requires delivery by an adenoviral vector that may itself elicit undesirable inflammatory effects.

Key regulators of radiation-induced apoptosis have been identified in salivary gland cells [Limesand et al., 2006; Matassa et al., 2001]. The expression of these pro-apoptotic genes is initiated by irradiation, eventually resulting in cell death. The delta isoform of protein kinase C (Pkcδ) is a ubiquitous enzyme, which is activated during the cellular apoptotic response to ionizing radiation. A salivary gland cell-specific, pro-apoptotic role of Pkcδ protein has also been described in irradiation experiments *in vitro* [Reyland et al., 1999]. Intriguingly, genetic disruption of the *Pkcδ* gene suppresses radiation-induced apoptosis in mouse parotid gland [Humphries et al., 2006] and protects serous acinar cells from radiation damage. Native Pkcδ is cleaved into its catalytically active form at the early phase of the apoptotic response by caspase-3, which is itself activated as a result of signals triggered by Bax in irradiated intestine epithelial cells [Thotala et al., 2010] and in lung cancer cells [Choi et al., 2006]. Bax is a pro-apoptotic member of the Bcl-2 protein family and mediates the intrinsic or "mitochondrial" pathway of programmed cell death in mouse parotid cells [Avila et al., 2009]. Accordingly, the absence of radiation-induced p53-dependent Bax expression in *p53* knockout mice provides radioprotection to salivary acinar cells. We hypothesized that direct silencing of these specific pro-apoptotic mediators could interfere with the apoptotic pathway and potentially facilitate salivary gland cell survival. We therefore tested whether transient siRNA-mediated inhibition of *Pkcδ* or *Bax* gene expression can protect against radiation damage of salivary gland cells. We report here the effects of radiation on salivary gland cells following the selective knock down of the pro-apoptotic *Pkcδ* and *Bax* genes.

The use of small (21–23bp), interfering RNAs (siRNA) for gene therapy is well-established. Synthetic, double-stranded RNAs have been applied to *in vivo* anti-cancer treatments, airway disease control, and liver regeneration. However, siRNA delivery to salivary gland cells and tissue has been less well studied. To date, siRNA transfections of salivary gland

cells have been accomplished using commercially available transfection reagents [Bulosan et al., 2009; Freitas et al., 2007]. Those reagents are designed for siRNA transfections in cell culture experiments, and their cytotoxicity might not be tolerated in vivo [Mahato et al., 2003]. As an alternative, we report on the pioneer application of a unique nanoparticle-based delivery system designed to carry siRNAs into salivary gland cells. These nanoparticles consist of novel, pH-sensitive diblock copolymers which bind to siRNAs electrostatically and protect them from degradation [Convertine et al., 2009]. Furthermore, the backbone of the nanocomplexes is formed from nonimmunogenic and nontoxic polymers [Benoit et al., 2011; Convertine et al., 2009; Convertine et al., 2010; Kusonwiriyawong et al., 2003]. We have assessed the capability of the nanoparticle complexes to deliver sequence-specific siRNA duplexes targeting pro-apoptotic genes into salivary gland cells.

Stable cell lines have been valuable in the investigation of acinar cell apoptosis [Limesand et al., 2003; Stephens et al., 1989], but the cellular response to radiation may be altered, as they are transformed cells. We have therefore conducted these investigations using primary cell cultures from mouse submandibular glands. Here we describe *in vitro* experiments to establish a radioprotection strategy through siRNA-mediated knock down of pro-apoptotic genes.

Materials and methods

Primary salivary gland cultures

Submandibular glands were aseptically excised from 2–4 month-old Balbc/cByJ mice, purchased from Jackson Laboratory (Bar Harbor, MA). The University Committee on Animal Resources at the University of Rochester approved all procedures and protocols. The glands were minced using a razor blade, then transferred into 10 ml digestion buffer prepared from $CaCl_2$ -/$MgCl_2$- Hanks' balanced salt solution with 16.7 mg dispase, 10mg collagenase type II (GibcoR Invitrogen, CA) and 40 mg hyaluronidase (Sigma, MO) [Hisatomi et al., 2004]. Enzymatic digestion was performed at 37°C for 90 minutes (fresh enzyme solution was added after the first 45 minutes) on a shaking rack. Further dissociation of the digested tissue was induced by vigorous pipetting prior to passing the cell suspension through a 40μm cell strainer (BD Falcon, NJ). The isolated cells were then plated onto fibronectin-laminin (Invitrogen) coated 6-well dishes (BD Falcon) in Williams' E medium (Gibco), supplemented with 10% (v/v) heat-inactivated fetal bovine serum (Gibco), epidermal growth factor (EGF) (20 ng/ml; Sigma), insulin (10 μg/ml, Invitrogen), dexamethasone (0.25μM, Invitrogen), antibiotic-antimycotic solution (1% v/v, Gibco), nicotinamide (2mM, Gibco), MEM-NEAA (1% v/v, Gibco), and ITS (1% v/v, Cellgro, VA). Cultures were incubated at 37°C in a humidified chamber of 5% (v/v) CO_2 in air. Growth media was changed every second day. To distinguish the major cell types in monolayer cultures, lineage specific markers [Kishi et al., 2006] were used and visualized by immunostaining. Immunocytochemical analysis of the cultured cells was carried out using anti-amylase (1:300, Santa Cruz Biotechnology, Santa Cruz, CA), anti-cytokeratin-19 (1: 100, Santa Cruz), and anti-sca-1(1:400, R&D Systems, Inc. Minneapolis, MN) antibodies.

Nanoparticle-siRNA transfections

Monolayers were grown to subconfluency and 24 hours prior to transfection the growth medium was changed to serum-free/antibiotic-free medium. A commercially available transfection reagent, Lipofectamine (Invitrogen) was used according to the manufacturer's protocol as a control method to check siRNA transfection efficiency. Transfection efficiency was visualized using an Alexa Fluor 555-labeled, dsRNA oligomer (Cy3 BLOCKiTFluControl, Invitrogen).

The preparation and characterization of the pH-responsive diblock copolymers and resultant nanoparticles has been published elsewhere [Benoit et al., 2010; Benoit et al., 2011; Convertine et al., 2009; Convertine et al., 2010]. Nanoparticle/siRNA complexes were formulated using the calculated amount of siRNAs from 5μM stock solutions. *Silencer*® Pre-designed siRNAs were purchased from Ambion (Applied Biosystems, MA USA) for Pkcδ (sense strand; CCGUCGUGGAGCCAUUAAAtt, antisense strand; UUUAAUGGCUCCACGACGGtt), Bax (sense strand; GGAUGAUUGCUGACGUGGAtt; antisense strand; UCCACGUCAGCAAUCAUCCtt), and for negative controls (validated, non-targeting siRNA sequences). The micellar charge ratio (positive charges of diblock polymers compared to negative charges in siRNA) of the complexes was 4:1, and the nanocomplexed siRNAs were added to monolayers at a final concentration of 40nM siRNA in reduced serum OptiMEM (Gibco) medium.

Flow cytometric analysis

For each assay, Cy3-labeled siRNA was complexed with Lipofectamine or nanoparticle carriers and added to cell monolayers. After incubation with siRNA for 8 hours the transfected cells were trypsinized and resuspended in PBS (with 2% FBS and 0.01% trypan blue). 10,000 cells were analyzed per sample on a BD LSR II instrument (BD Biosciences, San Jose, CA). Gating was determined using untreated control samples.

Irradiation

In vitro gamma irradiation was performed with a Cs^{137} radiation source. To determine the optimal radiation dosage for transfection experiments, subconfluent monolayer cultures were irradiated with 1, 5, 7.5, or 10Gy. Two days following the irradiation, the survival rate of the salivary primary cells was determined for each dose using the trypan blue (Gibco) exclusion assay, and an initial dose response curve was calculated. For the radioprotection experiments, twenty four hours after transfection with siRNA, culture dishes containing siRNA/nanoparticle complex-treated samples or irradiation control (no transfection) samples were subjected to a single dose of 7.5Gy irradiation.

RNA isolation and gene expression analysis by quantitative PCR (qPCR)

Total RNA was isolated from monolayer cultures using the RNeasy Mini Kit (Qiagen, Germany). Primary cell cultures from untreated control wells, transfected wells, and irradiated wells were harvested 24 hours following treatment (in replicate). RNA concentration was calculated from the OD_{260}/OD_{280} absorption ratio using a SmartSpec Plus (Bio-Rad Laboratories, CA USA) spectrophotometer. Real time PCR analysis was completed in two steps. The cDNA transcription step was performed with the iScript cDNA Synthesis Kit (Bio-Rad) following the manufacturer's instructions. Quantitative PCR reactions were set up in 25μl IQ SYBR Green Supermix (Bio-Rad) total volume, containing the templates (0.5μg) and target-specific primer pairs. The nucleotide sequences for primers were designed using information from the GenBank database (http://www.ncbi.nlm.nih.gov/Genbank) and are listed in Table 1. Quantification of the transcripts was performed using the CFX96 Real-Time System (Bio-Rad) with the following cycling parameters: pre-incubation (95°C for 10 min), 45 cycles of amplification (denaturing at 95°C for 15 s, annealing at 62°C for 30 s, and elongation at 72°C for 30 s), and melting curve analysis with continuous fluorescent measurement. Standard curves from a control dilution series were created, and pro-apoptotic gene expression levels were normalized to three reference genes (UBC, ubiquitin; GAPDH, glyceraldehyde-3-phosphate dehydrogenase; S18, ribosomal protein [Silver et al., 2008]).

Western blot

Monolayer cultures were harvested using ice-cold RIPA lysis buffer (G-Biosciences, MO) with protease inhibitor cocktail tablets (Complete Mini, Roche, Germany). Cells were incubated at 95°C for 5 min in 4x-Laemmli's buffer (200mM Tris-HCl, 400mM β-mercaptoethanol, 8% SDS, 0.2% bromophenol blue, 40% glycerol; all reagents were analytical grade materials from Sigma). The lysate protein concentration was assayed using the BCA (Pierce, IL) method. Fifteen μg protein were separated by SDS–PAGE gel electrophoresis on 4–15%% (w/v) acrylamide gels (RGEL, Bio-Rad). Separated proteins were transferred onto PVDF membrane (ImmobilonP, Millipore, MA) with a wet system. After rinsing and blocking (5% dried skim milk in TBS) the blots were incubated with the primary antibodies: Pkcδ rabbit polyclonal antibody 1:500 (cs-213, Santa Cruz), Bax rabbit polyclonal antibody 1:300 (cs-493, Santa Cruz), and β-actin mouse monoclonal antibody 1:1000 (sc-47778, Santa Cruz). Secondary antibodies were goat anti-rabbit IgG-HRP (cs-2004, Santa Cruz) and goat anti-mouse IgG-HRP (cs-200, Santa Cruz), respectively. The proteins were visualized by enhanced chemiluminescence (ECL Plus, Amersham, UK) according to the manufacturer's instructions. Alpha image scanning of the blots was done to measure the difference in band intensity among samples and quantification was performed using ImageJ Basics (NIH) analysis software.

Apoptosis detection

Radiation induced cellular apoptosis was assessed by the visualization of apoptotic changes in specific compartments of the cells 24 hours after ionizing radiation of primary cultures. All of the procedures were performed in 6-well dishes following the manufacturer's instructions.

Nuclear: in situ detection of apoptotic cells within the monolayer culture was achieved using the DeadEnd Fluorometric TUNEL System (Promega, WI USA). The fragmented DNA was labeled by fluorescein-12-dUTP and the apoptotic cells were visualized by fluorescence microscopy.

Cytosol: endogenous caspase-3 activation was detected with SignalStain Cleaved Caspase-3 detection kit (Cell Signaling, MA USA). The kit contains cleaved caspase-3 antibody, which binds to a biotinylated secondary antibody and is detected using the avidin-biotin complex system.

Mitochondrial: Early apoptotic changes in living cells were detected using the Mitocapture Apoptosis Detection Kit (BioVision, CA USA). Mitochondrial disruption leads to altered mitochondrial potential and red aggregates of a cationic dye can be visualized in the cytoplasm by fluorescence microscopy.

Statistical analysis

Experimental data were analyzed using the one-way ANOVA method followed by appropriate post hoc tests (Dunnett's or Tukey's HSD). Values are presented as mean values ± standard deviation. *P*-values <0.05 were considered statistically significant results. Statistical analyses were performed using the SPSS (PASW Statistics 18) software for Windows.

Results

pH-responsive nanoparticles deliver siRNA into primary salivary gland cells in vitro

Mouse submandibular glands were dissociated and grown in monolayer culture, as described [Hisatomi et al., 2004]. After 48 hours in culture, all non-attached clumps and cells were

removed, and within five days, colonies of cells were expanded. To assess cell types present in the cultures, cells were fixed with 4% paraformaldehyde, and subjected to immunostaining using antibodies specific for acinar (amylase, Fig.1B), and duct (cytokeratin 19, Fig.1C) cells, as well as a stem cell marker-1 (sca-1, Fig.1D). We observed subsets of cells that reacted with each marker.

To evaluate transfection efficiency, we first tested the ability of the pH-responsive nanoparticles to deliver fluorescently tagged siRNA into monolayer cultures, using Cy3-labeled siRNA molecules. siRNAs were complexed either with nanoparticles or Lipofectamine at 37°C, added to cell monolayers in 6-well plates and incubated for 6 hours. Examination by fluorescence microscopy (excitation max = 547nm, emission max = 563nm) showed that a majority of the cells were labeled with Cy3-tagged siRNA (Fig.1G, H). Cellular incorporation of the nanocomplexes showed efficiency similar to Lipofectamine positive controls (Fig.1G), and confirmed the delivery of siRNAs into target cells. Intracellular uptake (Fig. 1I, J) of siRNA/nanoparticle complexes was quantified in cultures; monolayers were treated with trypsin and subjected to flow cytometric analysis based on Cy3 fluorescence (Fig. S1). Cy3-positive cells in Lipofectamine and nanoparticle-mediated transfections represented 83.6% (±6.75% SD) and 78.9% (±2.7%) of the total cell number, respectively.

Nanoparticle/ siRNA complexes mediate efficient knock down of Pkcδ and Bax

To test the ability of the internalized siRNAs to knock down gene expression, we used siRNAs designed to target the Pkcδ or Bax proteins. The efficacy of nanoparticle complexes for siRNA delivery was established in a previous investigation [Benoit et al., 2010]. Experiments with various nanoparticle/siRNA charge ratios established that the most potent micellar charge ratio is 4:1 to achieve optimized particle size and surface charge. At this particular charge ratio, the polymers are complexed to siRNAs to provide effective cellular uptake and subsequent gene knock down.

At 24 hours after siRNA/ nanoparticle addition, cell lysates were prepared and analyzed by qPCR, as well as on Western blots. Functional knock down of Pkcδ or Bax was assessed in whole cell extracts using immunoblotting techniques. Parallel positive controls used a commercially available siRNA carrier (Lipofectamine-2000) for knock down. qPCR measurement of mRNA levels showed that Pkcδ and Bax expression levels were significantly decreased (45.7% ± 2.5%, and 52.1% ± 1.7%, respectively) in the presence of nanocomplexed siRNA (Fig. 2A, B). Furthermore, the expression of both Pkcδ (Fig. 2C) and Bax (Fig. 2D) proteins were significantly reduced as compared to cells receiving the scrambled siRNA controls. Relative to the mock control, Pkcδ and Bax protein expression was suppressed (48.8% ± 18%, and 49.4% ± 8.0%, respectively) in the presence of nanoparticle/siRNA complexes (Fig. 2E, F). As the level of gene knock down with nanoparticle-bound siRNAs was similar to that obtained in the positive transfection controls with Lipofectamine, all subsequent experiments were accomplished using nanocomplexed siRNAs.

Pro-apoptotic gene knock-down in irradiated salivary gland cells

To characterize the radiosensitivity of the cultured primary submandibular gland cells, it was necessary to establish a dose response curve representative for the actual experimental conditions (e.g. radiation source, cell culture protocol) [Konings et al., 2005]. Monolayer cultures were exposed to increasing doses of γ-ionizing radiation from 0 to 10 Gy and the overall cell viability was determined 48 hours following irradiation. Floating and trypsinized adherent cells were loaded into the counting chamber of a hemocytometer and dead cells, which take up trypan-blue, were counted. Cell survival, expressed as the percentage of

unstained (viable) cells to the total number of cells, in Figure 3A, showed a dose-dependent decrease with increasing radiation. The 7.5Gy single dose irradiation resulted in a significant ($P < 0.05$), 40% reduction in cell survival. All subsequent radioprotection experiments were performed using this dosage.

We next evaluated the nanoparticle/siRNA complexes for their ability to mediate target gene silencing of *Pkcδ* or *Bax* following radiation treatment, *in vitro*. At 24 hours after a single 7.5Gy irradiation, measurement of mRNA expression levels by qPCR showed that the *Pkcδ* gene expression in the irradiated samples was decreased to background levels equal to those in non-transfected and non-irradiated controls (Fig 3B; Pkcδ expression decreased by 44.4% ± 14.4% in Pkcδ siRNA/ nanoparticle-treated wells compared to scrambled siRNA/ nanoparticle-treated controls). Bax mRNA expression was also significantly reduced (Fig. 3C; 31.6% ± 3.8%). Furthermore, protein expression analysis of the nanoparticle/siRNA treated cultures, conducted at 24 hours after irradiation (Fig 3D, E), confirmed the qPCR mRNA results. Pkcδ and Bax proteins were decreased by 65.81% ± 6.7%, and 31.9% ± 16.2%, respectively in the siRNA/nanoparticle-treated wells.

siRNAs targeted to pro-apoptotic genes confer resistance to radiation-induced apoptosis of cultured salivary gland cells

To test whether the demonstrated knock down of *Pkcδ* or *Bax* expression confers functional radioprotection, primary cultures from submandibular glands were prepared and treated with Pkcδ or Bax siRNA/nanoparticle complexes. All cultures were subjected to a single dose of radiation 24h after transfection (7.5Gy). Radiation induced-damage was assessed at 24 hours, using three independent assays for apoptosis.

The intrinsic apoptosis pathway involves the activation of caspase-3 protein, which occurs as part of the early response to radiation. 7.5Gy ionizing radiation resulted in a 3-fold increase of caspase-3 activity in monolayers of irradiation controls (Fig. 4B, E), before the subsequent DNA fragmentation (Fig. 5B, E). siRNA-mediated gene silencing of both *Pkcδ* and *Bax* with nanoparticle complexes led to an attenuated apoptotic response in cultured cells. Caspase-3 staining decreased by 60% ± 19% in Pkcδ or Bax siRNA/nanoparticle-treated wells compared to those treated with scrambled siRNA/nanoparticles (Fig.4C-E). Furthermore, mitochondrial membrane disruption, as determined by the number of Mitocapture-positive cells, was decreased by 65.8 ± 15% and 52.6% ± 15% in Pkcδ or Bax siRNA/nanoparticle-treated wells, respectively, compared to scrambled siRNA/nanoparticle control wells (Fig. 4F). Analysis using TUNEL also showed a reduced number of apoptotic cells following siRNA/nanoparticle-mediated knock down of Pkcδ or Bax (Fig. 5A–D). Counts of TUNEL-positive cells scored as apoptotic were determined in each sample and are compared in Fig. 5E. A significant decrease in the number of TUNEL-positive cells was apparent in Pkcδ or Bax siRNA/nanoparticle-treated wells, (50.0 ± 10.5% and 40.6% ± 11.8%) respectively, compared to scrambled siRNA-treated or control wells. Trypan blue staining confirmed that the percentage of surviving cells was increased following pro-apoptotic gene knock down (Fig. 5F).

Discussion

Radioprotection is an important goal for improving the clinical management of head and neck cancer patients [Mehanna et al., 2010]. We hypothesized that the targeted knock down of genes involved in the apoptotic response to radiation could result in the protection of these cells from cell death. This notion was based on earlier reports demonstrating that knockout of the *Pkcδ* gene, an essential regulator of apoptosis in epithelial cells, results in suppression of apoptosis of primary salivary gland cells following irradiation [Humphries et al., 2006]. Furthermore, the inhibition of Pkcδ activity by a specific antagonist, rottlerin,

suppresses apoptosis in immortalized salivary cells [Reyland et al., 1999]. Therefore, we initiated gene silencing experiments with siRNAs targeting two pro-apoptotic genes, *Pkcδ* and *Bax*, known to be involved in radiation-induced salivary gland damage. The use of siRNAs to silence pro-apoptotic genes is critical, since reversibility of the knock down may be particularly important when apoptotic pathways are targeted, to avoid altering essential downstream signaling pathways.

Potential strategies for radioprotection of the salivary glands must be developed using methods that are compatible with *in vivo* applications. In this report, we have employed a novel type of nanocarrier to enhance siRNA internalization into target cells. The nanoparticles have previously been tested *in vitro* and found to have no cytotoxic effects in a cell culture system [Convertine et al., 2009; Convertine et al., 2010]. We have employed the nanoparticles to deliver siRNAs to primary salivary gland cells, in order to target pro-apoptotic gene expression in a non-invasive and transient manner. The nanoparticles are less than 50nm in diameter, and include a pH-responsive endosomolytic component that promotes the release of the siRNA from endosomes into the cytoplasm, following cellular uptake. According to Segura and Hubbell [2007], properly selected particle size (maximum of 200nm) and surface charge (slightly positively charged) are critically important to promote intracellular uptake into the target cells. The nanoparticle/siRNA preparations used in our experiments conform to these parameters. The siRNAs are non-covalently complexed with the biodegradable nanoparticles. Previous studies by Benoit et al. [2010] have demonstrated that these carrier biomolecules are capable of inducing siRNA-mediated knock down of target genes in ovarian cancer cells *in vitro*. Here, we show that nanoparticle-mediated delivery of Cy3-labeled siRNA into primary submandibular gland cultures is highly efficient (almost 80%), and that the fluorescent particles are evenly dispersed among the cells in our monolayer culture. The efficiency of cellular uptake into our primary cultures is slightly lower than the reported transfection level (90%) of HeLa cells achieved with the same type of nanoparticles [Benoit et al., 2011], and may reflect transfection differences between primary and established cell cultures. In the primary salivary gland cells used in this study, the knock down efficiencies achieved with the nanoparticles are equivalent to those achieved with the Lipofectamine transfection reagent.

The primary goal of this study was to address the feasibility of conferring radioprotection through siRNA-mediated gene knock down. Thus, prior to siRNA transfection experiments, the primary cultured salivary gland cells were measured for their susceptibility to radiation-induced damage. The radiosensitivity of the primary cell cultures demonstrated dose dependency similar to previously published reports on salivary acinar cell cultures, and to *in vivo* radiation treatment of salivary glands [Tateishi et al., 2008]. We therefore performed irradiations at a dose (7.5Gy) that is consistent both with other published studies using salivary gland cells [O'Connell et al., 1998; Vissink et al., 1992], and with exposure levels used in radiotherapeuticprotocols for human tumors [Dahlberg et al., 1999]. Our approach to determine apoptotic cell death in irradiated monolayers was adopted from O'Connell et al. [1998], thus only attached cells were used for apoptosis measurements. We used three independent assays to determine the effects of silencing Pkcδ and Bax protein expression on radiation-induced apoptosis. All three revealed a significant protective effect on irradiated salivary gland cell monolayers after targeting Pkcδ or Bax proteins. Quantification revealed a statistically significant reduction from 40 to 60% in the rate of apoptosis. A similar (~50%) reduction of apoptosis in an immortalized salivary cell line was demonstrated using Nox1- siRNA/oligofectamine transfections [Tateishi et al., 2008].

Our experiments confirm that RNAi-mediated inhibition of key apoptotic genes contributes to protection against irradiation-induced cell death *in vitro*. However, functional knock down of pro-apoptotic genes established in these experiments does not necessarily mean that

cell survival will be increased. A recent study on radiation-induced gastrointestinal damage [Kirsch et al., 2010] suggested that selective deletion of the pro-apoptotic p53 gene may radiosensitize cells, which implies that in addition to apoptosis, other mechanisms are involved in radiation damage. Moreover, interactive apoptotic routes complicate existing radiation injury models; Pkcδ as an apoptotic effector may stimulate the upstream Bax gene, thus enhancing apoptotic stimuli in the cell [Sitailo et al., 2004]. The current lack of knowledge on the network of cellular responses triggered by radiation complicates the elaboration of prevention strategies and damage control, and underscores the need to better understand the molecular mechanisms involved in radiation-induced cell killing.

In the development of a model for the investigation of radiation injury, it has been suggested that damage in the mouse salivary gland, characterized by inflammatory lesions, is similar to that in human glands [Urek et al., 2005]. We intentionally used primary cultures of mouse salivary gland tissue in our experiments, because we believe this provides a superior *in vitro* model for salivary gland responses to irradiation when compared to immortalized or cancer-derived salivary gland cell lines. Indeed, primary cultures of mouse submandibular glands are a heterogeneous cell population that includes the major functional cell types present in normal tissue (acinar, ductal and stem cells). Furthermore, primary cell cultures provide a more valid model for the variability in gene delivery and gene knock down efficiency that is likely to occur *in vivo* [Chen et al., 2005], although, in the absence of the innate immune system, the *in vitro* response to apoptotic stimulus may be intensified [Riss and Moravec, 2004]. Thus, *in vivo* studies will be required to establish this potential strategy for preventing radiation damage by targeting pro-apoptotic genes.

In summary, we have tested nanoparticle-based delivery of siRNA into salivary gland primary cultures and have demonstrated successful target gene knock down. Moreover, pro-apoptotic gene silencing using siRNA and nanoparticle complexes was able to confer protection against the irradiation-induced apoptotic response. These findings have significant potential for future development of a treatment to promote radioprotection of the salivary glands in patients with head and neck cancer.

Supplementary Material

Refer to Web version on PubMed Central for supplementary material.

Acknowledgments

Contract grant sponsor: NIDCR

Contract grant number: R21 DE19302 to Steve Dewhurst and Catherine E. Ovitt

References

Avila JL, Grundmann O, Burd R, Limesand KH. Radiation-Induced Salivary Gland Dysfunction Results From p53-Dependent Apoptosis. International Journal of Radiation Oncology*Biology*Physics. 2009; 73:523–529.

Benoit DS, Henry SM, Shubin AD, Hoffman AS, Stayton PS. pH-responsive polymeric sirna carriers sensitize multidrug resistant ovarian cancer cells to doxorubicin via knockdown of polo-like kinase 1. Mol Pharm. 2010; 7:442–55. [PubMed: 20073508]

Benoit DS, Srinivasan S, Shubin AD, Stayton PS. Synthesis of folate-functionalized RAFT polymers for targeted siRNA delivery. Biomacromolecules. 2011; 12:2708–14. [PubMed: 21634800]

Braam PM, Terhaard CH, Roesink JM, Raaijmakers CP. Intensity-modulated radiotherapy significantly reduces xerostomia compared with conventional radiotherapy. Int J Radiat Oncol Biol Phys. 2006; 66:975–80. [PubMed: 16965864]

Bulosan M, Pauley KM, Yo K, Chan EK, Katz J, Peck AB, Cha S. Inflammatory caspases are critical for enhanced cell death in the target tissue of Sjogren's syndrome before disease onset. Immunol Cell Biol. 2009; 87:81–90. [PubMed: 18936772]

Chen AA, Derfus AM, Khetani SR, Bhatia SN. Quantum dots to monitor RNAi delivery and improve gene silencing. Nucleic Acids Res. 2005; 33:e190. [PubMed: 16352864]

Choi SY, Kim MJ, Kang CM, Bae S, Cho CK, Soh JW, Kim JH, Kang S, Chung HY, Lee YS, Lee SJ. Activation of Bak and Bax through c-abl-protein kinase Cdelta-p38 MAPK signaling in response to ionizing radiation in human non-small cell lung cancer cells. J Biol Chem. 2006; 281:7049–59. [PubMed: 16410245]

Convertine AJ, Benoit DS, Duvall CL, Hoffman AS, Stayton PS. Development of a novel endosomolytic diblock copolymer for siRNA delivery. J Control Release. 2009; 133:221–9. [PubMed: 18973780]

Convertine AJ, Diab C, Prieve M, Paschal A, Hoffman AS, Johnson PH, Stayton PS. pH-Responsive Polymeric Micelle Carriers for siRNA Drugs. Biomacromolecules. 2010

Dahlberg WK, Azzam EI, Yu Y, Little JB. Response of human tumor cells of varying radiosensitivity and radiocurability to fractionated irradiation. Cancer Res. 1999; 59:5365–9. [PubMed: 10537321]

Eriksson D, Stigbrand T. Radiation-induced cell death mechanisms. Tumour Biol. 2010; 31:363–72. [PubMed: 20490962]

Freitas VM, Vilas-Boas VF, Pimenta DC, Loureiro V, Juliano MA, Carvalho MR, Pinheiro JJV, Camargo ACM, Moriscot AS, Hoffman MP, Jaeger RG. SIKVAV, a Laminin [alpha]1-Derived Peptide, Interacts with Integrins and Increases Protease Activity of a Human Salivary Gland Adenoid Cystic Carcinoma Cell Line through the ERK 1/2 Signaling Pathway. Am J Pathol. 2007; 171:124–138. [PubMed: 17591960]

Grundmann O, Mitchell GC, Limesand KH. Sensitivity of salivary glands to radiation: from animal models to therapies. J Dent Res. 2009; 88:894–903. [PubMed: 19783796]

Hisatomi Y, Okumura K, Nakamura K, Matsumoto S, Satoh A, Nagano K, Yamamoto T, Endo F. Flow cytometric isolation of endodermal progenitors from mouse salivary gland differentiate into hepatic and pancreatic lineages. Hepatology. 2004; 39:667–75. [PubMed: 14999685]

Humphries MJ, Limesand KH, Schneider JC, Nakayama KI, Anderson SM, Reyland ME. Suppression of apoptosis in the protein kinase Cdelta null mouse in vivo. J Biol Chem. 2006; 281:9728–37. [PubMed: 16452485]

Jensen SB, Pedersen AM, Vissink A, Andersen E, Brown CG, Davies AN, Dutilh J, Fulton JS, Jankovic L, Lopes NN, Mello AL, Muniz LV, Murdoch-Kinch CA, Nair RG, Napenas JJ, Nogueira-Rodrigues A, Saunders D, Stirling B, von Bultzingslowen I, Weikel DS, Elting LS, Spijkervet FK, Brennan MT. A systematic review of salivary gland hypofunction and xerostomia induced by cancer therapies: management strategies and economic impact. Support Care Cancer. 2010; 18:1061–79. [PubMed: 20333412]

Kirsch DG, Santiago PM, di Tomaso E, Sullivan JM, Hou WS, Dayton T, Jeffords LB, Sodha P, Mercer KL, Cohen R, Takeuchi O, Korsmeyer SJ, Bronson RT, Kim CF, Haigis KM, Jain RK, Jacks T. p53 controls radiation-induced gastrointestinal syndrome in mice independent of apoptosis. Science. 2010; 327:593–6. [PubMed: 20019247]

Kishi T, Takao T, Fujita K, Taniguchi H. Clonal proliferation of multipotent stem/progenitor cells in the neonatal and adult salivary glands. Biochem Biophys Res Commun. 2006; 340:544–52. [PubMed: 16376857]

Konings AW, Coppes RP, Vissink A. On the mechanism of salivary gland radiosensitivity. Int J Radiat Oncol Biol Phys. 2005; 62:1187–94. [PubMed: 15990024]

Kusonwiriyawong C, van de Wetering P, Hubbell JA, Merkle HP, Walter E. Evaluation of pH-dependent membrane-disruptive properties of poly(acrylic acid) derived polymers. Eur J Pharm Biopharm. 2003; 56:237–46. [PubMed: 12957638]

Lee HJ, Lee YJ, Kwon HC, Bae S, Kim SH, Min JJ, Cho CK, Lee YS. Radioprotective effect of heat shock protein 25 on submandibular glands of rats. Am J Pathol. 2006; 169:1601–11. [PubMed: 17071584]

Limesand KH, Barzen KA, Sanders LA, Sclafani RA, Raynolds MV, Reyland ME, Anderson SM, Quissell DO. Characterization of rat parotid and submandibular acinar cell apoptosis in primary culture. In Vitro Cell Dev Biol Anim. 2003; 39:170–7. [PubMed: 14505429]

Limesand KH, Said S, Anderson SM. Suppression of radiation-induced salivary gland dysfunction by IGF-1. PLoS One. 2009; 4:e4663. [PubMed: 19252741]

Limesand KH, Schwertfeger KL, Anderson SM. MDM2 is required for suppression of apoptosis by activated Akt1 in salivary acinar cells. Mol Cell Biol. 2006; 26:8840–56. [PubMed: 16982679]

Mahato RI, Henry J, Narang AS, Sabek O, Fraga D, Kotb M, Gaber AO. Cationic lipid and polymer-based gene delivery to human pancreatic islets. Molecular therapy : the journal of the American Society of Gene Therapy. 2003; 7:89–100. [PubMed: 12573622]

Matassa AA, Carpenter L, Biden TJ, Humphries MJ, Reyland ME. PKCdelta is required for mitochondrial-dependent apoptosis in salivary epithelial cells. J Biol Chem. 2001; 276:29719–28. [PubMed: 11369761]

Mehanna H, Paleri V, West CM, Nutting C. Head and neck cancer--Part 1: Epidemiology, presentation, and prevention. BMJ. 2010; 341:c4684. [PubMed: 20855405]

Nagler R, Marmary Y, Fox PC, Baum BJ, Har-El R, Chevion M. Irradiation-induced damage to the salivary glands: the role of redox-active iron and copper. Radiat Res. 1997; 147:468–76. [PubMed: 9092927]

Nagler RM. The enigmatic mechanism of irradiation-induced damage to the major salivary glands. Oral Dis. 2002; 8:141–6. [PubMed: 12108758]

O'Connell AC, Lillibridge CD, Zheng C, Baum BJ, O'Connell BC, Ambudkar IS. γIrradiation-induced cell cycle arrest and cell death in a human submandibular gland cell line: Effect of E2F1 expression. Journal of Cellular Physiology. 1998; 177:264–273. [PubMed: 9766523]

O'Connell AC, Redman RS, Evans RL, Ambudkar IS. Radiation-induced progressive decrease in fluid secretion in rat submandibular glands is related to decreased acinar volume and not impaired calcium signaling. Radiat Res. 1999; 151:150–8. [PubMed: 9952299]

Redman RS. On approaches to the functional restoration of salivary glands damaged by radiation therapy for head and neck cancer, with a review of related aspects of salivary gland morphology and development. Biotech Histochem. 2008; 83:103–30. [PubMed: 18828044]

Reyland ME, Anderson SM, Matassa AA, Barzen KA, Quissell DO. Protein kinase C delta is essential for etoposide-induced apoptosis in salivary gland acinar cells. J Biol Chem. 1999; 274:19115–23. [PubMed: 10383415]

Riss TL, Moravec RA. Use of multiple assay endpoints to investigate the effects of incubation time, dose of toxin, and plating density in cell-based cytotoxicity assays. Assay Drug Dev Technol. 2004; 2:51–62. [PubMed: 15090210]

Segura T, Hubbell JA. Synthesis and in vitro characterization of an ABC triblock copolymer for siRNA delivery. Bioconjug Chem. 2007; 18:736–45. [PubMed: 17358044]

Seiwert TY, Salama JK, Vokes EE. The chemoradiation paradigm in head and neck cancer. Nat Clin Pract Oncol. 2007; 4:156–71. [PubMed: 17327856]

Silver N, Cotroneo E, Proctor G, Osailan S, Paterson KL, Carpenter GH. Selection of housekeeping genes for gene expression studies in the adult rat submandibular gland under normal, inflamed, atrophic and regenerative states. BMC Mol Biol. 2008; 9:64. [PubMed: 18637167]

Sitailo LA, Tibudan SS, Denning MF. Bax activation and induction of apoptosis in human keratinocytes by the protein kinase C delta catalytic domain. J Invest Dermatol. 2004; 123:434–43. [PubMed: 15304079]

Stephens LC, Schultheiss TE, Price RE, Ang KK, Peters LJ. Radiation apoptosis of serous acinar cells of salivary and lacrimal glands. Cancer. 1991a; 67:1539–43. [PubMed: 2001542]

Stephens LC, Schultheiss TE, Price RE, Ang KK, Peters LJ. Radiation apoptosis of serous acinar cells of salivary and lacrimal glands. Cancer. 1991b; 67:1539–1543. [PubMed: 2001542]

Stephens LC, Schultheiss TE, Small SM, Ang KK, Peters LJ. Response of parotid gland organ culture to radiation. Radiat Res. 1989; 120:140–53. [PubMed: 2798777]

Takagi K, Yamaguchi K, Sakurai T, Asari T, Hashimoto K, Terakawa S. Secretion of saliva in X-irradiated rat submandibular glands. Radiat Res. 2003; 159:351–60. [PubMed: 12600238]

Tateishi Y, Sasabe E, Ueta E, Yamamoto T. Ionizing irradiation induces apoptotic damage of salivary gland acinar cells via NADPH oxidase 1-dependent superoxide generation. Biochem Biophys Res Commun. 2008; 366:301–7. [PubMed: 18035043]

Thotala DK, Geng L, Dickey AK, Hallahan DE, Yazlovitskaya EM. A new class of molecular targeted radioprotectors: GSK-3beta inhibitors. Int J Radiat Oncol Biol Phys. 2010; 76:557–65. [PubMed: 20117291]

Thula TT, Schultz G, Tran-Son-Tay R, Batich C. Effects of EGF and bFGF on irradiated parotid glands. Ann Biomed Eng. 2005; 33:685–95. [PubMed: 15981868]

Urek MM, Bralic M, Tomac J, Borcic J, Uhac I, Glazar I, Antonic R, Ferreri S. Early and late effects of X-irradiation on submandibular gland: a morphological study in mice. Arch Med Res. 2005; 36:339–43. [PubMed: 15950071]

Vissink A, Down JD, Konings AW. Contrasting dose-rate effects of gamma-irradiation on rat salivary gland function. Int J Radiat Biol. 1992; 61:275–82. [PubMed: 1351916]

Vissink A, Jansma J, Spijkervet FK, Burlage FR, Coppes RP. Oral sequelae of head and neck radiotherapy. Crit Rev Oral Biol Med. 2003; 14:199–212. [PubMed: 12799323]

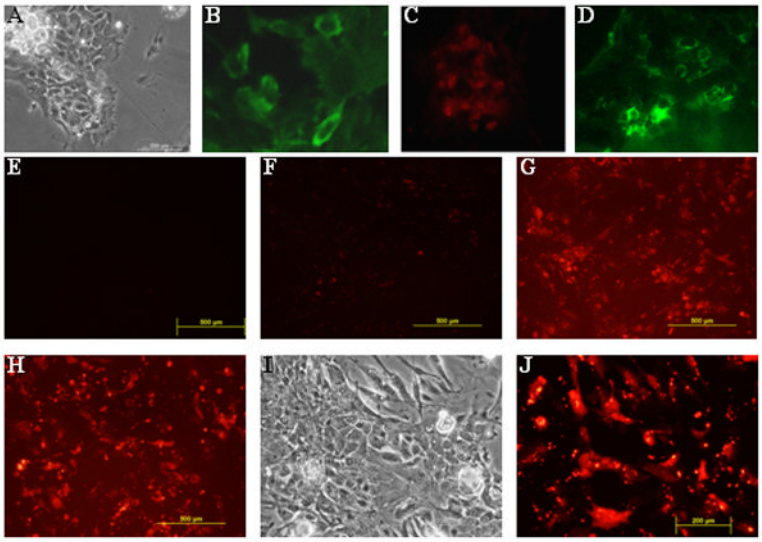

Figure 1.

Primary cell cultures derived from mouse submandibular gland include major cell types. A, phase contrast image of a monolayer culture. Representative photomicrographs of salivary gland specific lineage markers: B, immunocytochemistry with antibody to α-amylase detects secretory acinar cells (green); C, immunocytochemistry with antibody to cytokeratin 19, a representative marker for differentiated duct cells (red); D, immunocytochemistry with antibody to sca-1, a marker reported to label the progenitor cells of the salivary gland (green). E, Cells treated with nanoparticles complexed to scrambled-siRNA show no fluorescence signal after transfection. F, In no vector transfections, fluorescent Cy3-labeled siRNA is not internalized and serves as a negative control. G, Lipofectamine-mediated delivery of Cy3-labeled siRNA (positive control) shows evenly distributed siRNA uptake after 8 hours. H, Nanoparticle-mediated Cy3-labeled siRNA shows similar level of distribution after 8 hours. I, Higher magnification phase contrast image and J, fluorescent image of the same cells showing cellular internalization of siRNA mediated by the pH-responsive nanoparticles.

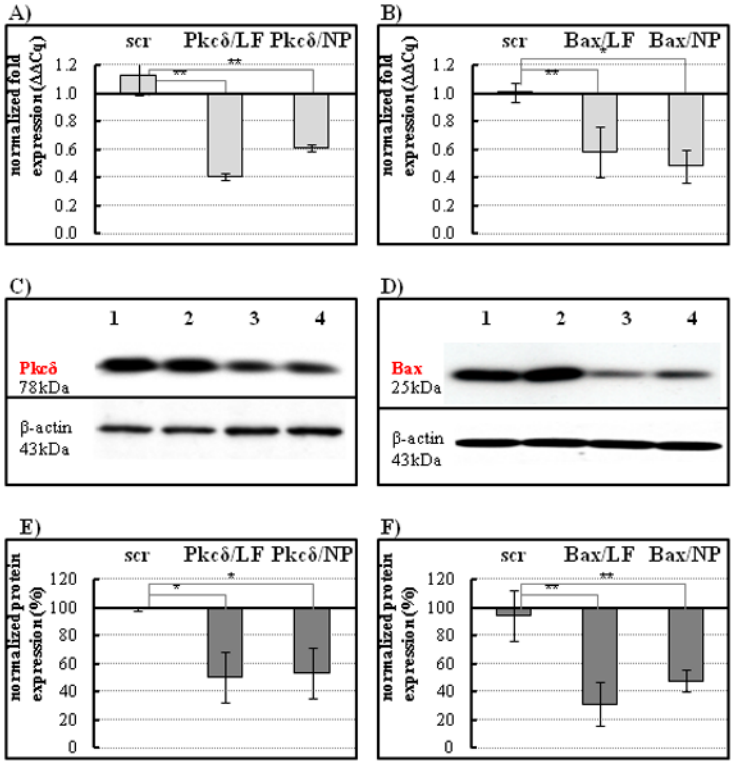

Figure 2.

siRNA knock down of Pkcδ or Bax expression in cultured salivary gland cells. A–B, mRNA expression was analyzed by qPCR 24 hours following transfection. A, Transfection with Pkcδ siRNA using Lipofectamine (LF) or nanoparticles (NP) inhibits Pkcδ mRNA expression compared to scrambled siRNA control (scr) delivered by nanoparticles; B, Transfection with Bax siRNA using Lipofectamine (LF) or nanoparticles (NP) demonstrated efficient reduction of Bax mRNA expression levels. Results are representative of three replicates and compared to untreated controls (fold changes); *P < 0.05 by one-way analysis of variance with Dunnett's multiple comparison test. C–D, The lysed cells were analyzed for expression levels of the two pro-apoptotic proteins on Western blots. C, Pkcδ, or D, Bax protein expression was normalized to β-actin (blots were stripped and reprobed). Lane 1, untreated cells; lane 2, cells treated with scrambled siRNA control; lane 3, cells treated with Lipofectamine-mediated siRNA, as positive control; lane 4, cells treated with nanoparticle-mediated siRNA. E–F, graphs show quantification of protein band intensities from Western blot analysis, scanned by alpha imaging and measured using the ImageJ (NIH) software. LF, Lipofectamine; NP, nanoparticle complexes. Calculations were based on three measurements compared to untreated controls (protein level established as 100%); *P < 0.05, **P< 0.001.

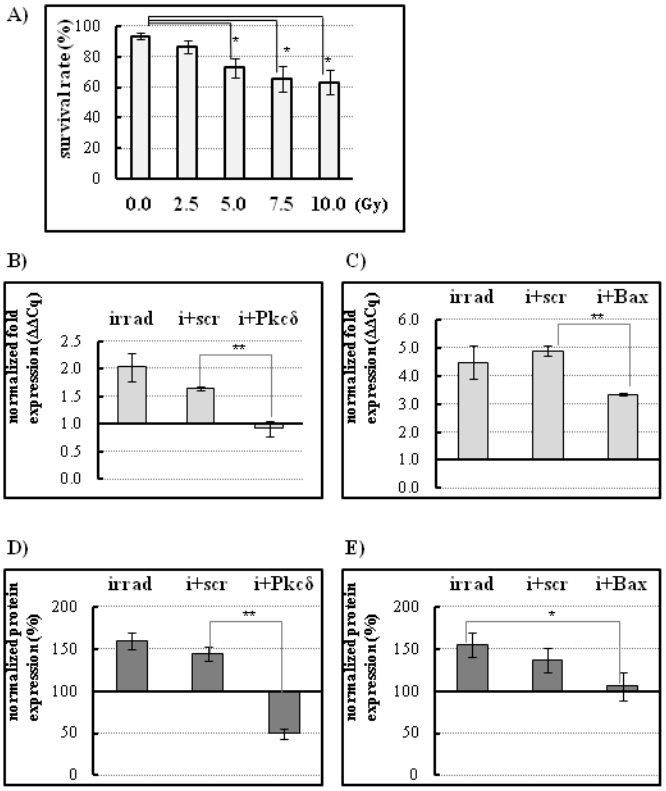

Figure 3.

siRNA knock down blocks radiation-induced increase of the pro-apoptotic genes Pkcδ or Bax. A, Dose response curve of irradiated salivary gland monolayer cultures. Cells were counted 24 hours after the indicated dose of γ-ray radiation. 7.5Gy single dose irradiation resulted in a significant ($P < 0.05$), 40% reduction in cell survival, and was used in all subsequent experiments. Radiation normally increases Pkcδ (B) or Bax (C) gene expression. However, nanoparticle-mediated siRNA knock down of Pkcδ or Bax expression blocks the radiation-induced increase. Cells were irradiated 24 hours after siRNA/nanoparticle addition, and mRNA levels were assayed by qPCR after an additional 24 hours. Results are representative of three replicates and compared to the untreated controls. D–E, Total protein extracts were analyzed by Western blot. Densitometric analysis of control and sample band ratios was conducted. The untreated control level of each protein was designated as 100%. D, Radiation-induced Pkcδ protein expression showed a statistically significant decrease in the presence of siRNA (i + Pkcδ) compared to the scrambled siRNA (scr) negative control. E, Radiation-induced Bax protein level was also reduced in cells in the presence of siRNA/nanoparticle complexes (i + Bax). (*$P < 0.05$, **$P<0.001$, $n=3$) Statistical significance was calculated using one-way analysis of variance with Tukey's multiple comparison tests.

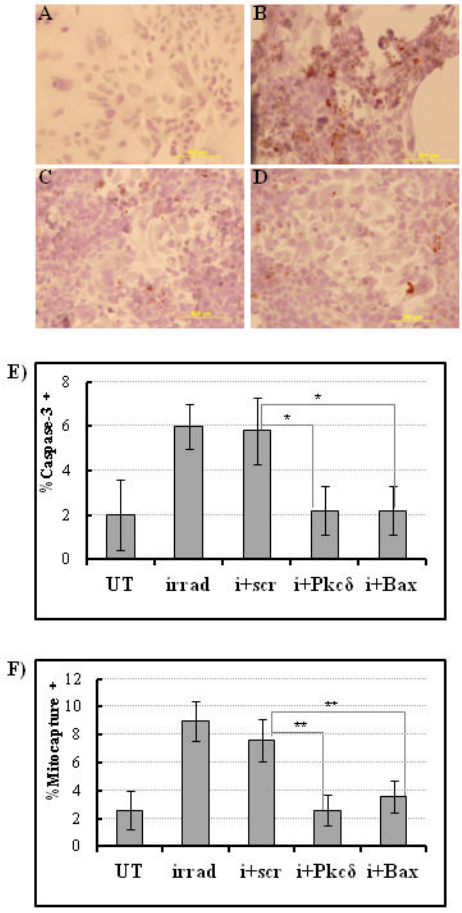

Figure 4.

Inhibition of pro-apoptotic Pkcδ or Bax protein expression decreases salivary gland cell sensitivity to radiation damage *in vitro*. A, Non-irradiated control cells stained with caspase-3 antibody and hematoxylin show no caspase-3 activity. B, Radiation treatment alone significantly increases caspase-3 activity in salivary gland monolayer cultures (caspase-3 positive cells are dark brown on hematoxylin counterstain). Pre-treatment with (C) nanoparticle/Pkcδ siRNA complexes or (D) nanoparticle/Bax siRNA complexes reduces caspase-3 staining in irradiated salivary gland cells compared to non-treated cells. E, Quantitative analysis of the caspase-3 staining based on cell counts within a defined region of the microscopic field. Percentage of caspase-3 positive cells is derived from number of caspase-3 positive cells/ total number of cells counted. UT, untreated control cells; irrad, irradiated cells; i+scr, irradiated cells pretreated with scrambled siRNA; i + Pkcδ or Bax, irradiated cells pretreated with siRNA to Pkcδ or Bax (n=5, *P < 0.05). F, Mitochondrial membrane disruption was determined using a Mitocapture assay 24 hours after irradiation (n=5 randomly chosen microscopic fields of each sample group) Percentage of mitocapture-positive cells is derived from # of mitocapture positive cells/ total # cells counted. UT, untreated cells; irrad, irradiated cells; i+scr, irradiated scrambled-siRNA treated cells; i+ Pkcδ, irradiated Pkcδ-siRNA treated cells; i+Bax, irradiated Bax-siRNA treated cells. **P<0.001. Statistical significance was tested by ANOVA and Tukey's multiple comparison tests.

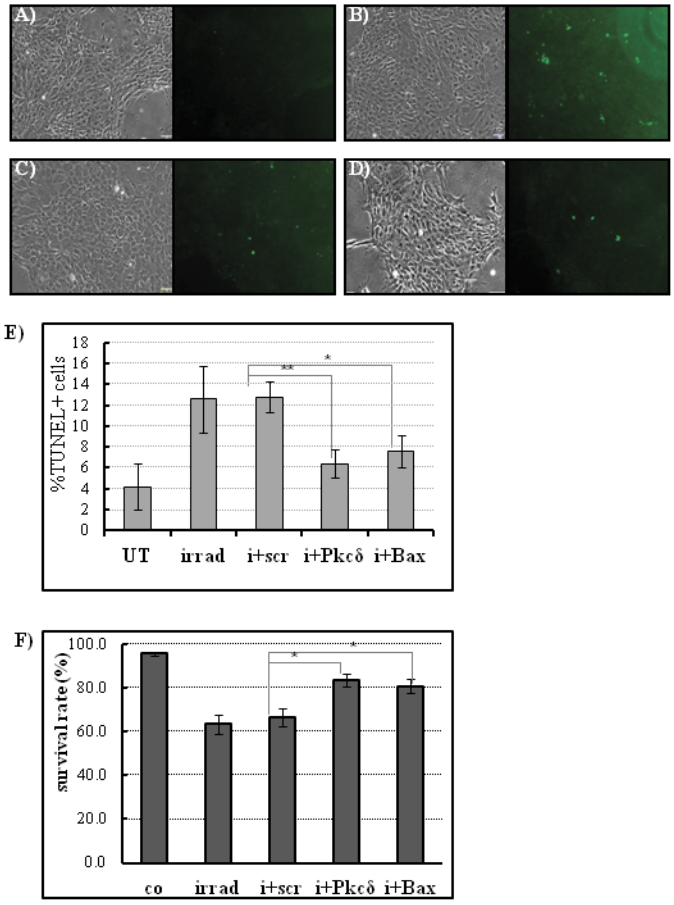

Figure 5.

siRNA knock down of Pkcδ or Bax expression reduces apoptotic cell death and increases radioprotection in irradiated primary salivary gland cells *in vitro*. A–D, Identical bright-field and fluorescent images of cell monolayers after TUNEL staining to detect apoptotic cells (green). A, Untreated cells have no detectable TUNEL-positive cells. B, Treatment with 7.5Gy radiation induces a significant increase in the number of apoptotic cells after 24 hours. C, Pretreatment with nanoparticle/ Pkcδ siRNA complexes before radiation treatment decreases the number of apoptotic cells. D, Pretreatment with nanoparticle/ Bax siRNA complexes before radiation treatment also decreases the number of apoptotic cells. E, Quantitative summary of TUNEL positive cells in control and siRNA-treated monolayers. Percentages represent TUNEL positive cells/total cells counted per microscopic field. UT, untreated control cells; irrad, irradiated cells; i+scr, irradiated cells pretreated with scrambled siRNA; i + Pkcδ or Bax, irradiated cells pretreated with siRNA to Pkcδ or Bax. F, Trypan blue staining confirms that the percentage of surviving cells was increased following pro-apoptotic gene knock down. Irradiation (7.5Gy) was performed 24 hours after pretreatment with nanoparticles complexed to Pkcδ or Bax siRNA, and live cells were counted on the following day using the Trypan-blue exclusion assay. (n=5, **P<0.001; Statistical significance was tested by ANOVA and Tukey's multiple comparison tests.) Overall cell numbers were determined using parallel phase contrast images. Co, untreated cells; irrad, irradiated cells; i+scr, irradiated scrambled-siRNA treated cells; i+ Pkcδ, irradiated Pkcδ-siRNA treated cells; i+Bax, irradiated Bax-siRNA treated cells).

Table I

qPCR primer sequences for reference and pro-apoptotic genes

Gene symbol	Forward (5'->3')	Reverse (5'->3')
UBC	AAGCCCCTCAATCTCTGGACGC	TCTCAATGGTGTCACTGGGCTCG
GAPDH	TGTGTCCGTCGTGGATCTGA	TTGCTGTTGAAGTCGCAGGAG
18S	ACGGAGGATGAGGTGGAGCGAGT	AAGTGGCCAGCCCTCTATGGG
Pkcδ	TCCTTCTCGGTGGACTGGTGGT	AAGAGCTCGTCCTCATCGTCGC
Bax	CCGGGTGGCAGCTGACATGTTT	GTAGAAGAGGGCAACCACGCGG